8

Digital Signal Processing and Artificial Intelligence Methods for Intracardial Signal Complexity Evaluation

Vaclav Kremen and Lenka Lhotska
Department of Cybernetics, Faculty of Electrical Engineering,
Czech Technical University in Prague
Czech Republic

1. Introduction

Advances in catheter ablation therapy have led to a widespread increase in its use in management of arrhythmias. The high success rates and low complication rates of this technique have revolutionized treatment of such conditions as Wolff-Parkinson-White syndrome, AV nodal reentrant tachycardia, and atrial tachycardia. More recently, catheter ablation has become a useful alternative to medical therapy in patients with atrial flutter and AF. Because these arrhythmias are among the most common seen in clinical practice and can at times be difficult to manage pharmacologically, primary care physicians need to be aware of new developments in treatment in order to offer an alternative to pharmacological therapy when it is contraindicated, ineffective, or poorly tolerated (Kosinski et al., 1998).
Since the milestone publication more than a decade ago by Haissaguerre et al (Haissaguerre et al., 2003) describing the role of ectopic foci within the pulmonary veins (PV), much progress has been achieved in the field of (potentially) curative ablation of atrial fibrillation. It is possible that the multiple linear lesions (ie, a mitral isthmus line, roofline) in addition to pulmonary vein isolation effectively modify AF substrate skin to a surgical Maze procedure. However, treating all chronic AF patients with an identical approach has one glaring weakness: Not all chronic AF patients are the same. Subjecting every patient to the same ablation set is not logical and likely results in many unnecessary lesions. The search for a new approach to identify target areas for AF ablation resulted in 2 new strategies in latest years: mapping of high-dominant-frequency areas and mapping of areas with stable complex fractionated atrial electrograms (CFAEs) (Nademanee, 2007). Mapping of CFAE as target sites for AF ablation has shown great promise (Nademanee et al., 2004). Nademanee et al. (Nademanee et al., 2004) concluded that CFAE areas represent critical sites for AF perpetuation and can serve as target sites for AF ablation (Kottkamp & Hindricks, 2007). Other works that showed new quantification measures of A-EGM during AF used morphological features of the atrial waves (Faes & Ravelli, 2007) in contrast to previously proposed measures to describe A-EGMs. In a recent study Scherr et al. (Scherr et al., 2007) showed the first use of an algorithm for automatic search of CFAEs and A-EGM complexity description in A-EGMs recorded during AF mapping procedures.
Nademanee et al. (Nademanee et al., 2004) sought to investigate the electrophysiological substrate and referred in their publication introduction to the work of Allessie's group. In

a landmark publication, Konings et al. (Konings et al., 1997) described high-density mapping of electrically induced AF in patients with Wolff-Parkinson-White syndrome undergoing surgery using a spoon-shaped electrode with 244 unipolar electrodes. In that study, the right atrium was investigated and was found to be activated by one or multiple wavelets propagating in different directions. Three types of right atrial activation during AF were identified. From type I to type III, the frequency and irregularity of AF increased, and the incidence of continuous electrical activity and reentry became higher (Konings et al., 1994). Electrogram morphology was found to be an indicator for collision of wavefronts (short double potentials), conduction block (long double potentials), and pivoting points or slow conduction (fragmented potentials) (Konings et al., 1997) and (Kottkamp & Hindricks, 2007). Unfortunately, mapping of high-dominant-frequency areas has been shown not to be effective in chronic AF patients (Sanders et al., 2005). On the other hand, mapping of CFAE as target sites for AF ablation has shown great promise (Nademanee et al., 2004). This approach is based on observations of several recent mapping studies in human AF. During sustained AF, CFAEs often are recorded in specific areas of the atria and exhibit surprisingly remarkable temporal and spatial stability (Nademanee et al., 2004) and (Jais et al., 1996) Nademanee et al. concluded (Nademanee et al., 2004) that CFAE areas represent critical sites for AF perpetuation and can serve as target sites for AF ablation (Kottkamp & Hindricks, 2007).
However, currently used algorithms still have some settings that need to be set up manually, so that execution of the algorithms are not fully automatic and it needs to be tested under a range of conditions. New stable algorithms for automatic evaluation of fibrillation electrograms are thus not only of scientific interest but can also provide a proper basis for selecting the most appropriate AF treatment (Kottkamp & Hindricks, 2007; Scherr et al., 2007). In 2007 and 2008 we developed a background methodology and techniques to extract more A-EGM features that are based on several possible information dimensions (degree of freedom) of the A-EGM signal, for example entropy, DF and CFAEs based features, as well as time and frequency domain analysis features. We introduced the unique wavelet transform based algorithm for searching fractionated segments (FSs) in A-EGM signal, sequentially followed by extraction algorithms that allow to mine the information of level of fractionation of the signal (A-EGM signal complexity) based on local electrical activity, which is automatically found by this algorithm (Křemen & Lhotská, 2007b). We described and tested more than 40 features, and based on several selection criteria we selected the most important 15 features that entered the sequential steps of features evaluation and A-EGM complexity classification/evaluation (Křemen & Lhotská, 2008). The major and methodological part of this work is presented here to uncover these new possibilities of artificial intelligence and signal processing of A-EGM for broader spectrum of electrophysiologists and cardiologists or scientists who are interested in this field of AF treatments.

2. Defining A-EGM classes of fractionation

First of all, we would like to make clear what kind of measurements and A-EGM signals we had at our disposal and we used for the analysis. All atrial bipolar electrograms used in this work were collected during left-atrial endocardial mapping using 4-mm irrigated-tip ablation catheter (NaviStar, Biosense-Webster) in 12 patients (9 males and 3 females, aged 56 ± 8 years) with persistent AF. The A-EGMs acquired before the ablation procedure were band-pass filtered ($30 - 400$ Hz) and sampled at frequency of 977 Hz by CardioLab 7000 (Prucka Inc.). Continuous recording from mapping catheter was exported in digital format, and subsequently split into 1500 ms segments exhibiting good endocardial contact, stable

signal pattern, and reasonable signal-to-noise ratio. A-EGM signals were stored and analyzed later in off-line regime manually by the experts.
All A-EGM signals preselected by the expert using the above described procedure were ready to be ranked by other experts into classes of fractionation (CF), which would reflect the level of fractionation of each individual A-EGM signal in dataset. This ranking was used in the study in next steps of A-EGM signal preprocessing, description (defining measures of A-EGM) and classification (see sections 3, 4, and 5).
Although the degree of fractionation of the A-EGM signals in the dataset, and also in reality, was assumed to be naturally continuous, a discrete set of CF was chosen for the purposes of study to be used by experts as ranking options. This was decided due to impossibility to classify signals by experts in smoother scale (the experts classified A-EGMs simply by looking at signal in time domain). From the same reason the ranking options were set up to four degree sets of classes of fractionation (four CF) for the purposes of the study. The four CF enabled to get a uniform dataset of A-EGMs with significant number of samples in each class, so that such dataset could be used in next steps in data processing, A-EGMs description and classification to get desirable statistical significance of results of experiments. These four CF were set up as ranking options for experts:

1. Organized activity – high percentage of organized signal activity in current signal (above 90 %).
2. Mild degree of fractionation – approximatelly same level of organized and disorganized activity of the signal.
3. Intermediate degree of fractionation – high percentage of disorganized activity of the signal (above 50%).
4. High degree of fractionation – disorganized A-EGM signal (highly fractionated).

Three independent experts were asked to assign each A-EGM signal in the dataset to one of four optional CF. The ranking was done manually by simply displaying an individual A-EGM signal from the dataset, looking at it in time domain (simulation of real-time mapping procedure) and assigning the signal to a considered CF. Custom written software developed for this purpose was programmed in software Matlab v.7 and it was used by each expert. The experts had the same information and condition to classify signals, which are commonly used during AF mapping procedure. They used A-EGM signal displayed on the screen followed bottom with ECG signal, captured from the same time as partial A-EGM signal, having possibility to switch between $I, aVF, V1, CS1.2, CS3.4, ABL1.2, ABL3.4$ and *Stim* inputs. The only difference from current clinical practice was no time pressure as during real-time mapping procedure and experts had enough time to evaluate or reevaluate individual A-EGMs.
After the experts ranked a displayed A-EGM signal, they switched to next one in the dataset. They could go through all ranked signals after they performed individual ranking and they had possibility to change the ranking for partial A-EGMs to make corrections at any time of ranking procedure. No specific criteria for signal assessment (e.g. dominant frequency or percentage of continuous electrical activity) were given. The experts were just asked to classify the A-EGMs by their subjective judgment according to how the ablation at particular site would be valuable for atrial debulking. The examples of the A-EGMs assigned by experts to class $1-4$ are shown in Figure 1.

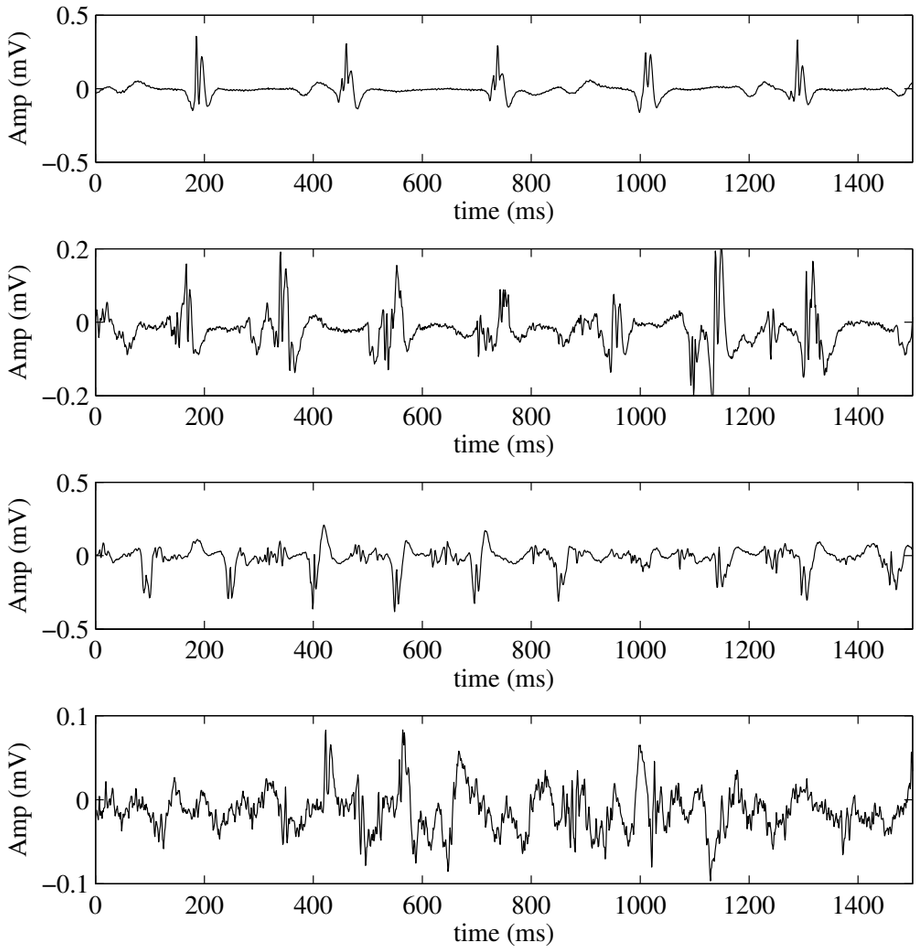

Fig. 1. Four complex fractionated atrial electrograms are shown. These are representatives of each CF used in the study. From the top to bottom:
1 – organized atrial activity,
2 – mild,
3 – intermediate,
4 – high degree of fractionation.

3. A-EGM signal preprocessing

Signal preprocessing plays a very important role for further A-EGM signal analysis and classification of level of fractionation of a given A-EGM signal. In this section the main problem which normally arises in signal processing task is described, namely signal denoising. The filtering methods will be presented as part of wavelet framework. Other filtering approaches, such as classical and adaptive filters (AR, ARMAX models (Gustafsson, 2000) etc.) were also tested and can be used for filtering of A-EGM, but for the presented tasks of A-EGM preprocessing and further features extraction the best results were achieved

by wavelet filtering methods. In this section, attention is focused on the application of wavelet transform and filters. A concrete denoising of A-EGM signal will be demonstrated.
Fundamental viewpoints of wavelet transform merely for terminology and notation conventions are presented as a background of the A-EGM preprocessing used during this application. More detailed information on this topic can be found in (Burrus, 1997; Daubechies, 1992).

3.1 Wavelet transform

The classical Fourier transform (FT) is not suitable if the signal has time varying frequency, i.e. the signal is non-stationary. This means that the FT tells whether a certain frequency component exists or not. This information is independent on where in time this component appears. It is possible to analyze any signal by using an alternative approach called wavelet transform (WT). WT analyzes the signal at different frequencies with different resolutions. WT is designed to give good time resolution and poor frequency resolution at high frequencies and good frequency resolution and poor time resolution at low frequencies (Novak, 2003). This approach makes sense especially when the signal at hand has high frequency components for short durations and low frequency components for long durations, which is the case in most biological signals, mainly EEG, EMG, ECG and also A-EGM. One example of the wavelet analysis of A-EGM of CF 1 is shown in Figure 2.

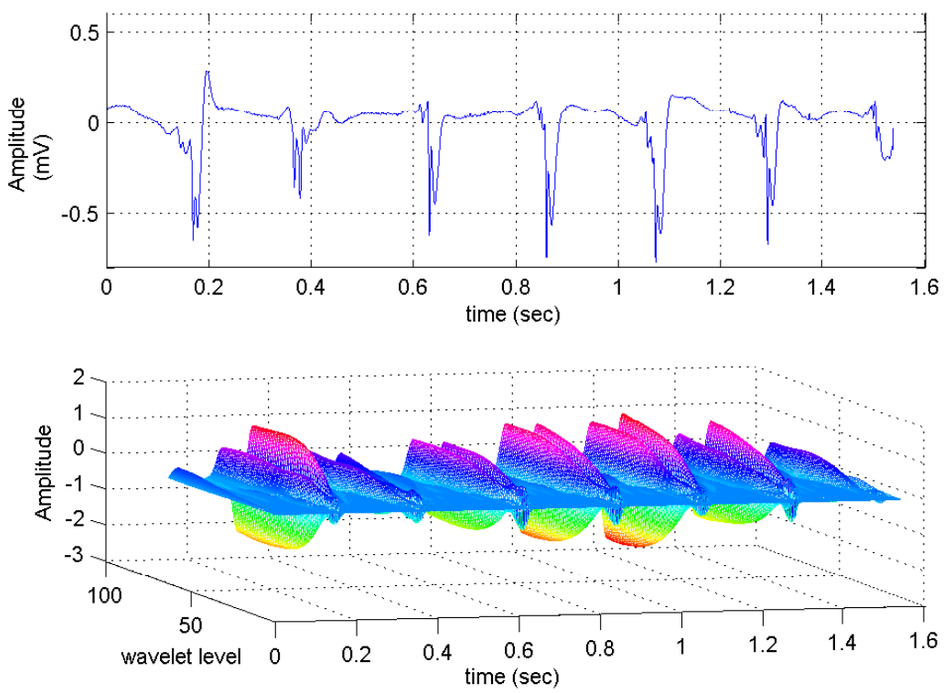

Fig. 2. Example of continuous Wavelet Transform (CWT) for A-EGM signal, which was ranked by three independent experts into class 1 – organized atrial activity. The A-EGM signal to be decomposed by CWT is shown at the top. Corresponding wavelet coefficients are depicted at the bottom.

3.2 Finalized A-EGM wavelet filter

In the described approach we used filtering (de-noising) of A-EGM signals performed using wavelet transform filter based on multilevel signal decomposition and thresholding of detailed coefficients (Mallat, 1999) described bellow. We found optimal filter setup by particle swarm optimization procedure (Křemen et al., 2007). The Coiflet of order four mother wavelet (MW) was used to decompose signal into 5 levels (Daubechies, 1992). Detail coefficients were thresholded by soft-thresholding (Donoho, 1995) with these settings of thresholds (level 1 (WT_{L1}) to level 5 (WT_{L5})): $0.02, 0.04, 0.008, 0.008, 0.008$. Reconstruction of the filtered signal was computed by wavelet reconstruction based on the original approximation coefficients and the modified detail coefficients of levels from 1 to 5.

Figure 3(a) shows a wavelet decomposition of A-EGM signal at 5 levels using Coiflet mother wavelet. From the Figure 3(a) subfigures a_1 and a_2 it is obvious that the main noise is focused in level 1 and 2 that corresponds to optimal filter thresholds setup found by optimization procedure (thresholds $WT_{L1} = 0.02$ and $WT_{L2} = 0.04$) (Křemen et al., 2007). Figure 3(b) shows the progression of described de-nosing procedure using optimal filter setup found by optimization procedure (Křemen et al., 2007). The optimal thresholds setup is used and depicted together with detailed coefficients before and after thresholding. The filtered signal shows the effectiveness of the filter that can be seen by watching the signal (Figure 4) or by comparing residuals in Figure 5.

Unfortunately, although using strong optimization particle swarm optimization procedure, some useful information for A-EGM classification was probably discarded during filtering process. This can be seen in analysis of residuals in Figure 5. The autocorrelation diagram of filtering residuals still shows some patterns, that are slightly correlated. It is obvious that these parts of the filtered signal are about tenth of amplitude of original signal in this partial example of the A-EGM signal which we are using here in this chapter for demostration of filtering. But although we used and tested more filtering approaches (classical filters, adaptive filters, wavelet filters) and strong optimization procedure, this effect of the filter could not be probably avoided. We concluded that the method outperformed the classical approaches as median or elliptic filters and that also after visual inspection the obtained results looked very clean which can be seen in Figure 4. This figure finally shows the example of original and filtered A-EGM signal to demonstrate the filtering efficacy in relation to visual aspects only.

4. A-EGM signal description - finding attributes

4.1 Basic concepts of feature construction

Before any modelling and classification of the signal takes place, a data representation must be chosen. In this chapter data is represented by a fixed number of features which can be binary, categorical or continuous. Feature is synonymous of input variable or attribute[1]. Finding a good data representation is very domain specific and related to available measurements. In A-EGM signal processing task, the "raw" data is represented by the matrix of A-EGM signals of 1.5 s length resampled at 1 kHz (section 2) and the extracted features (measures of A-EGM signal) that will be described in this section. That is, a set of variables of A-EGM signal that

[1] It is sometimes necessary to make the distinction between "raw" input variables and "features" or "measures" of signal that are variables constructed from the original input variables. Original input variables are in that case time series of amplitudes of the signal or other representation of this time domain signal (for example frequency spectrum of the A-EGM or wavelet representation of A-EGM). We will make it clear when this distinction is necessary.

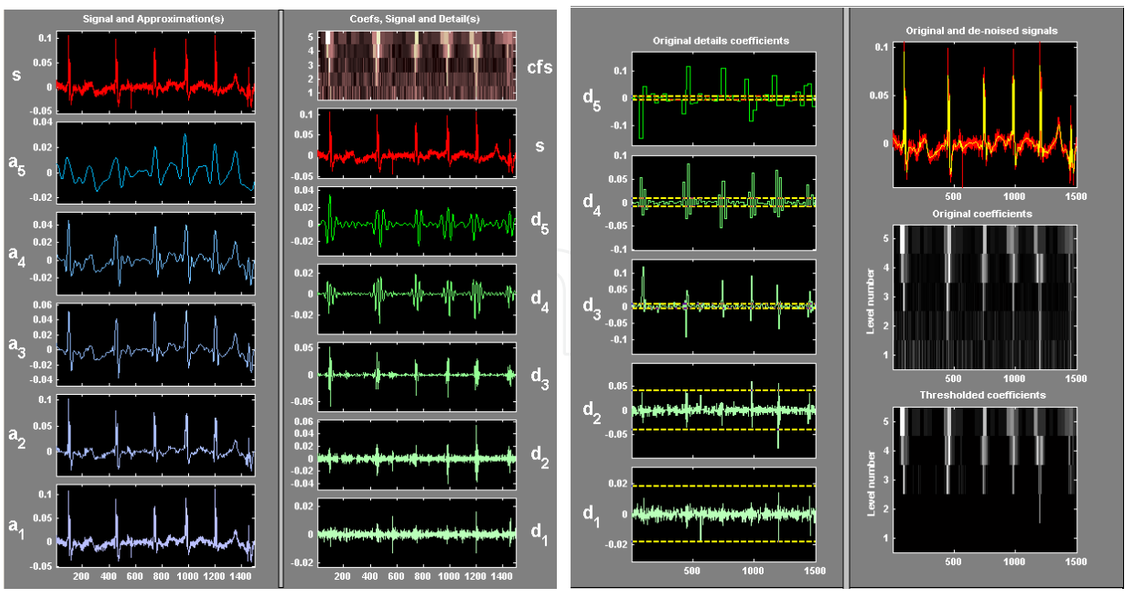

(a) Wavelet decomposition of A-EGM signal of CF 1.

(b) Wavelet denoising of A-EGM signal of CF 1

Fig. 3. (a) Wavelet decomposition of A-EGM signal, ranked by experts into CF 1. Decomposition at 5 levels was used performed with Coiflet of order four mother wavelet. Approximations and details are shown. From approximations and details of level 1 and 2 it is obvious that the main noise is focused in level 1 and 2, which corresponds to filter thresholds setup.
(b) Wavelet denoising of the same A-EGM signal shown on (a). The original signal is depicted in red and the filtered signal in yellow color. Decomposition at 5 levels was used and performed with Coiflet of order four mother wavelet. Thresholding of the detailed coefficients at 5 levels was performed to de-noise the signal. Dashed yellow lines show the values of individual optimal thresholds at all levels.

enable to categorize the A-EGM complexity (continually or to discrete classes of fractionation $1-4$).

4.2 Measurement of intervals between discrete peaks

The extraction of this A-EGM feature (measure) is based on an algorithm that works in time domain and calculates index of fractionation of A-EGM as a mean of the intervals between discrete peaks of A-EGMs (Figure 6), which are detected using input parameters of the algorithm: peak-to-peak sensitivity, signal width and refractory period. Input parameters of this algorithm were found by exhaustive search ($10x10$ validation) using measured dataset of A-EGM. The finally used optimal settings of the algorithm are: sensitivity $=$ 0.2 mV, signal width $=$ 8 ms, refractory period $=$ 14 ms. The feature is refereed to as MIDP in the chapter. This algorithm was first introduced by (Křemen et al., 2008).

4.3 Features based on description of local activation waves found automatically in A-EGM

These algorithms for A-EGM features extraction were developed in frame of this new methodology of A-EGM processing we introduce here. It enables to describe A-EGM

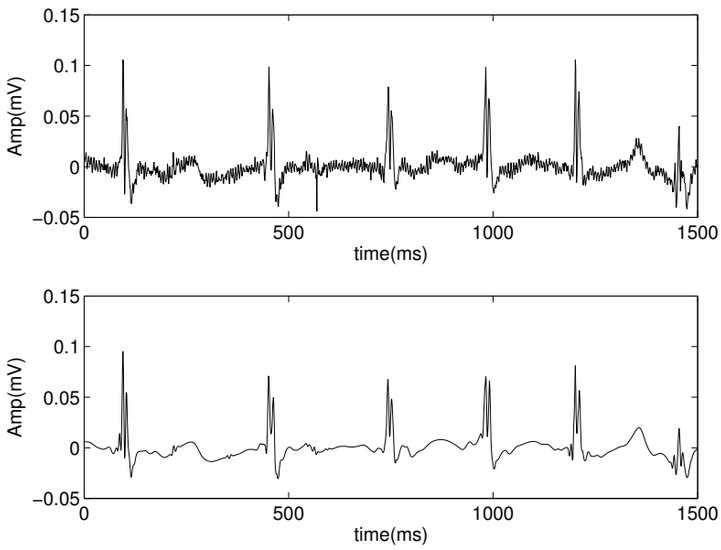

Fig. 4. The original (top) and filtered (bottom) A-EGM signal of CF 1. The filtering was performed by described wavelet filter.

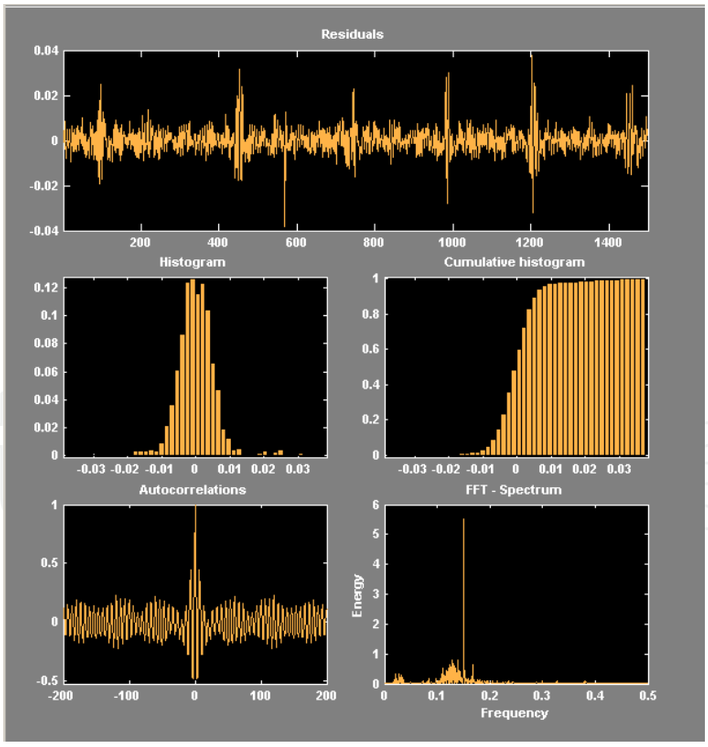

Fig. 5. The analysis of residuals after wavelet denoising procedure using described filter for A-EGM signal of CF 1. The residuals and autocorrelation diagrams show that some information about segments of local activation in A-EGM was filtered out with noise even in the best found "optimal" filter setup.

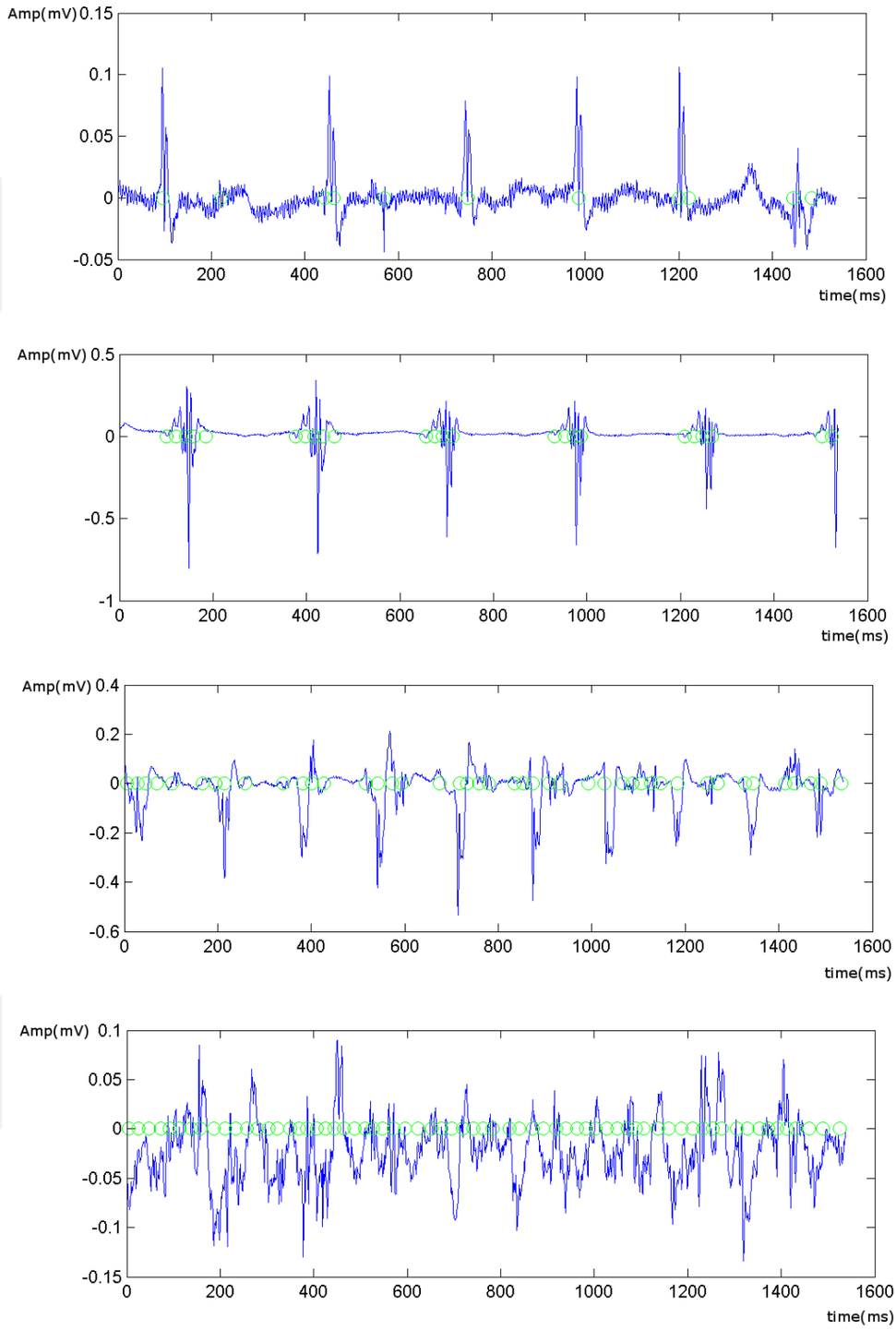

Fig. 6. The A-EGM representatives of each defined CF from cleared dataset are shown (from class 1 to class 4 from the top to bottom). Green circles show found discrete peaks of the signal defined by sensitivity 0.02 mV, signal width 8 ms and refractory period 14 ms in each A-EGM.

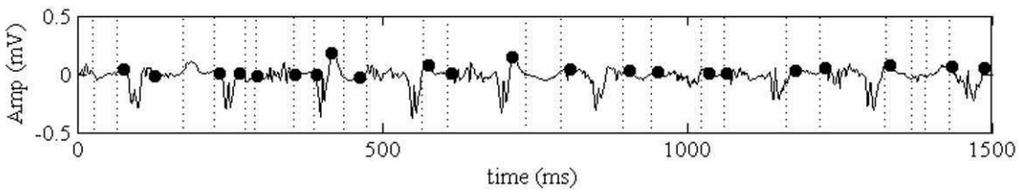

Fig. 7. Original A-EGM signal recorded during AF mapping procedure of persistent AF captured in left atria. Experts' ranking of the signal was into CF 3. Black dots denote the beginnings and the ends of FSs marked manually by expert to made a gold standard for comparison and optimizing of FSs searching algorithms. Dashed lines denote the beginnings and the ends of FSs found automatically by WTA.

complexity in a new way. The algorithms perform several automatic signal preprocessing steps. Based on this preprocessing, the algorithms then automatically search for areas of the A-EGM signal, where local electrical activity is found (areas of interest – fractionated segments (FSs), see Figure 7), also described by Faes et al. as local activation waves (LAWs) (Faes et al., 2007) and (Faes & Ravelli, 2007). Several features of A-EGM are then defined based on automatic FSs description. The features are therefore derived from the characteristics of the automatically observed FSs or LAWs.

Algorithm for automatic searching FSs

Fist we describe the algorithm for automatic searching FSs and then derived extraction of defined A-EGM measures. The problem of searching FSs is similar to problems of adaptive segmentation of the signal. The aim is to find the best algorithm that searches automatically (without need of a supervisor) for local electrical activity in the A-EGM signal to find FSs in that signal (Figure 7). We tried to approach the A-EGM signal in time domain only and also tried to find other adaptive segmentation methods suitable for this task, but the results were significantly worse than the results produced by the novel algorithm (Křemen & Lhotská, 2007b; 2008) that used a wavelet decomposition. We introduce this algorithm here very briefly. The algorithm searched for segments with local electrical activity (FSs) within A-EGMs (Figure 8a). The denoised signal (Figure 8b) was decomposed by discrete wavelet transform multilevel decomposition into 5 levels using the Coiflet wavelet of order 4. The detailed coefficients of the signal were reconstructed at level 3 (L_3). L_3 was normalized to its maximum absolute value (Figure 8c) and thresholded at 0.014 (A_T) (Figure 8d). All parts of the signal with non-zero absolute amplitude were set to arbitrary value of 1 denoting primary FSs (Figure 8e). Secondary FSs were defined as all nests of adjacent primary FSs with intersegment space $<$ 5 ms (T_T). The individual steps of the algorithm are shown in Figure 8. The parameters of this algorithm (type of mother wavelet, decomposition level L_3, thresholds A_T, and T_T) were found by particle swarm optimization technique (Křemen & Lhotská, 2007a). The individual steps of the algorithm are thoroughly shown in (Křemen & Lhotská, 2007b) and (Křemen & Lhotská, 2008). The algorithm is refereed to as WTA (wavelet transform algorithm) here.

New A-EGM measures defined

We designed this WTA as the basic preprocessing algorithm that serves to automatically search through measured A-EGM signal to find FSs in that signal. Based on these found

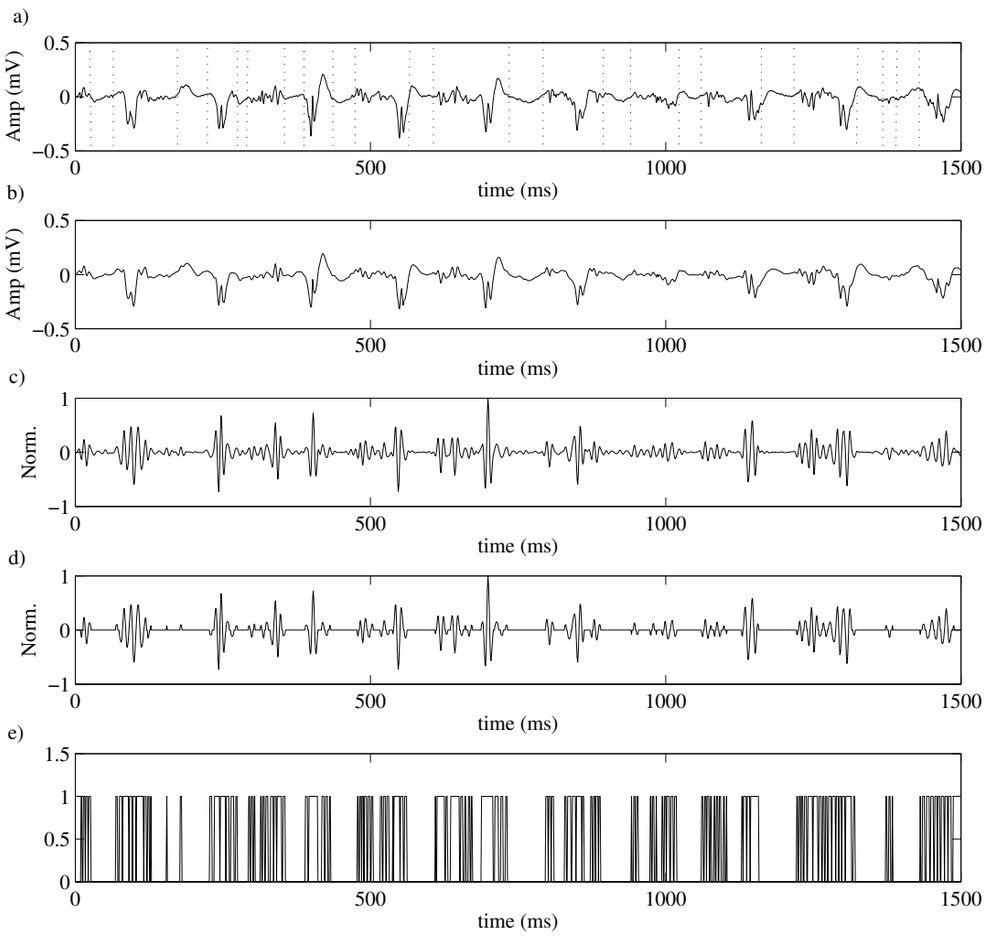

Fig. 8. a) De-noised A-EGM signal, assigned by three experts to class 3 is filtered by proposed wavelet filtering algorithm (b). The filtered signal entered the algorithm to find the individual FSs in that signal. c) Level 3 of the detailed coefficients of the discrete wavelet transform normalized with respect to its absolute maximal value. This signal was used to identify the individual FSs of the original A-EGM signal. d) The signal from c) thresholded by threshold value 0.014. e) The individual signal peaks (primary FSs) are marked by value 1. The peaks show areas of interest, where local electrical activity is visible. These peaks are joined/merged by threshold 5 ms to form areas of individual FSs (secondary FSs). The beginnings and ends of the automatically observed FSs are marked by dashed lines.

FSs we can define then several statistically dependent or independent features of A-EGM. We describe these individual features here briefly. To introduce these features we often use the statistical measures that are commonly known. We also tested other statistical measures, such as weighted mean etc., but they did not give such good results in A-EGM classification, therefore we did not introduce them here.

Number of fractionated segments

We defined a feature FS as a number of fractionated segments found by WTA in particular A-EGM signal in the dataset.

Statistical description of inflexion points in FSs

Number of Inflection Points calculated in automatically found FSs in A-EGM was defined as the new feature IPFS. We also defined four new features based on statistical analysis of IPFS in current one A-EGM signal:

- **MINIPFS** – Minimum of Inflection Points in found FSs in a particular A-EGM signal.
- **MAXIPFS** – Maximum of Inflection Points in found FSs in a particular A-EGM signal.
- **MIPFS** – Arithmetical Mean value of Inflection Points added together in automatically found FSs and calculated as $\bar{x} = 1/N \cdot \sum_{i=1}^{N} x_i$, where x_i is a number of inflection points in one FS number i, and N is total number of FS in particular A-EGM.
- **SDIPFS** – We used Standard Deviation of Inflection Points added together in automatically found FSs and calculated as $\sigma = \sqrt{1/N \cdot \sum_{i=1}^{N} (x_i - \bar{x})^2}$, where x_i is a number of inflection points in one FS number i, and N is total number of FS in particular A-EGM.

Statistical description of Zero level crossing points in FSs

Number of Zero level crossing points (the points where the signal changes the sign or the polarity) calculated in automatically found FSs in A-EGM was used as the new feature ZCPFS. We defined four new features based on statistical analysis of ZCPFS in current one A-EGM signal:

- **MAXZCPFS** – Maximum of Zero level Crossing Points in found FSs.
- **MINZCPFS** – Minimum of Zero level Crossing Points in found FSs.
- **MZCPFS** – Arithmetical Mean value of Zero level Crossing Points added together in automatically found FSs and calculated as $\bar{x} = 1/N \cdot \sum_{i=1}^{N} x_i$, where x_i is a number of inflection points in one FS number i, and N is total number of FS in particular A-EGM.
- **SDZCPFS** – We used Standard Deviation of Zero level Crossing Points added together in automatically found FSs and calculated as $\sigma = \sqrt{1/N \cdot \sum_{i=1}^{N} (x_i - \bar{x})^2}$, where x_i is a number of inflection points in one FS number i, and N is total number of FS in particular A-EGM.

Statistical description of inter-segment distance of FSs

The new feature was defined and calculated as total length of all inter-segment distances in particular A-EGM and refereed to as TDFS. We defined two new features based on statistical analysis of inter-segment distance of automatically found FSs in A-EGM signal:

- **MDFS** – Arithmetical Mean value of inter-segment distance of automatically found FSs calculated as $\bar{x} = 1/N \cdot \sum_{i=1}^{N} x_i$, where x_i is the inter-segment distance i of two corresponding FSs, and N is total number of inter-segment distances found automatically in particular A-EGM.
- **SDDFS** – We used Standard Deviation of inter-segment distance of automatically found FSs calculated as $\sigma = \sqrt{1/N \cdot \sum_{i=1}^{N} (x_i - \bar{x})^2}$, where x_i is the inter-segment distance i of two corresponding FSs, and N is total number of inter-segment distances found automatically in particular A-EGM.

Statistical description of width of FSs

This new feature was defined as sum of width of all FSs found in particular A-EGM, refereed to as TWFS. We also defined four new features based on statistical analysis of the widths of automatically found FSs in A-EGM signal:

- **MINWFS** – Minimal width of found FSs in particular A-EGM signal.
- **MAXWFS** – Maximal width of found FSs in particular A-EGM signal.
- **MWFS** – Arithmetical Mean value of widths of automatically found FSs calculated as $\bar{x} = 1/N \cdot \sum_{i=1}^{N} x_i$, where x_i is the width of one FS i, and N is total number of FSs found automatically in particular A-EGM.
- **SDWFS** – We used Standard Deviation of widths of automatically found FSs calculated as $\sigma = \sqrt{1/N \cdot \sum_{i=1}^{N} (x_i - \bar{x})^2}$, where x_i is the width of one FS i, and N is total number of FSs found automatically in particular A-EGM.

Statistical description of maxima of amplitude in FSs

Three new features were defined based on statistical analysis of maxima of amplitudes in automatically found FSs in A-EGM signal:

- **MAXAFS** – Maximal absolute value of Amplitude in found FSs in particular A-EGM signal.
- **MAFS** – Arithmetical Mean value of maximal absolute value of Amplitude in automatically found FSs calculated as $\bar{x} = 1/N \cdot \sum_{i=1}^{N} x_i$, where x_i is the maximal absolute value of amplitude in one FS number i, and N is total number of FSs found automatically in particular A-EGM.
- **SDAFS** – We used Standard Deviation of maximal absolute value of Amplitude in automatically found FSs calculated as $\sigma = \sqrt{1/N \cdot \sum_{i=1}^{N} (x_i - \bar{x})^2}$, where x_i is the maximal absolute value of amplitude in one FS number i, and N is total number of FSs found automatically in particular A-EGM.

Mean interval of peaks found in FSs

We used the features described in Section 4.2 and calculated the same features only for automatically found fractionated segments. We therefore acquired four new features:

1. **MIDPFS** – Mean of the Intervals between Discrete Peaks of A-EGM in found FSs.
2. **FIDPFS** – Mean of Intervals between Discrete Peaks using filtered A-EGM signals and in found FSs.

3. **NIDPFS** – Mean of Intervals between Discrete Peaks using normalized A-EGM signals and in found FSs.
4. **FNIDPFS** – Mean of Intervals between Discrete Peaks using filtered and normalized A-EGM signals and in found FSs.

Joining features MIDP & FIP & IPFS

We aggregated two features MIDP and IPFS into one MIDP&IPFS feature using simple formula: MIDP&IPFS = $\sqrt{MIDP^2 + IPFS^2}$, and next two features FIP and IPFS into new feature FID&IPFS by adding: FIP&IPFS = FIP + IPFS.

Measurement of morphological regularity and similarity of FSs

As showed by Faes et al., a morphological variations of the consecutive atrial depolarization waves (FSs or LAWs) can be described by an automated algorithm (Faes et al., 2007) and (Faes & Ravelli, 2007). Faes et al. also showed that atrial activity has a repetitive characteristics and regularity of present LAWs during organized atrial rhythms (flutter or type I AF) and on the contrary, highly disorganized electrograms showing fragmented LAWs with complex morphology contain more dissimilar LAWs, thus leading to zero the probability to find similar depolarizations (Faes & Ravelli, 2007). The algorithms describing the morphological similarity thus could play an important role to describe A-EGM complexity. We suggested and implemented a simple algorithm, which automatically describes the morphological similarity of automatically found FSs in individual A-EGM from used datasets.
The WTA algorithm was first used to find the FSs in currently processed A-EGM. Let's consider A-EGM signal $\mathbf{x}$ of length N, where $\mathbf{x} = [x_1, x_2, ...x_N]$. The FSs found by WTA in A-EGM signal $\mathbf{x}$ can be written as $\mathbf{y}$, where $\mathbf{y} = [\mathbf{y}_1, \mathbf{y}_2, ...\mathbf{y}_m]$, where m is the number of found FSs. We performed the estimate of cross-correlation of $\mathbf{x}$, and all vectors in $\mathbf{y}$. One cross-correlation of $\mathbf{x}$ and $\mathbf{y}_i$, where $i \in (1, m)$ was defined as:

$$\widehat{\mathbf{R}}_{xy_i}(m) = \begin{cases} \sum_{n=0}^{N-m-1} x_{n+m} y^*_{i_n} & m \geq 0 \\ \widehat{\mathbf{R}}^*_{xy_i}(-m) & m < 0 \end{cases} \quad (1)$$

If length of $\mathbf{y}_i$ was less than N, the vector $\mathbf{y}_i$ was zero padded to number of samples N.
The sequence $\widehat{\mathbf{R}}_{xy_i}$ was then normalized with respect to its absolute maxima, therefore normalized cross-correlation of $\mathbf{x}$ and $\mathbf{y}_i$ was calculated as: $\widehat{\mathbf{R}}'_{xy_i} = \widehat{\mathbf{R}}_{xy_i} / max|\widehat{\mathbf{R}}_{xy_i}|$. Thresholding of $\widehat{\mathbf{R}}'_{xy_i}$ was used to found the segments, where the higher correlation of $\mathbf{x}$ and $\mathbf{y}_i$ is present. Threshold $\delta = 0.7$ was find by particle swarm optimization procedure (Křemen & Lhotská, 2007a) to set to zero the segments of $\widehat{\mathbf{R}}'_{xy_i}$ with less correlated $\mathbf{x}$ and $\mathbf{y}_i$:

$$\widehat{\mathbf{R}}'_{xy_i}(m) = \begin{cases} \widehat{\mathbf{R}}'_{xy_i}(m) & \delta \geq 0.7 \\ 0 & \delta < 0.7 \end{cases} \quad (2)$$

The correlation peaks were found in $\widehat{\mathbf{R}}_{xy_i}(m)$ and determined as a index of morphological similarity ρ.
The performance of the algorithm could be adjusted by using more sophisticated approach that could be object of separate investigation (e.g. using of time warping methods etc.), but we are not describing it here in the chapter.

5. A-EGM signal classification

To determine the generalization ability of a model one would need to measure the average risk for the set of all possible data objects. In real life applications it is not feasible, so we estimated the risk using a test set. When doing this we should be aware of the danger of testing models on a single test set (for example resulting from a rigid partition of the set of all available data to the training and test parts). Model selection based on testing trained models on a single test set does not get rid of the danger of overfitting. A more accurate estimation of the empirical risk can be obtained with K-fold cross-validation (Guyon et al., 2006). In this technique we split the set of available data into n parts and perform n training and test processes (each time the test set is one of the parts and the training set consists of the rest of the data). The average test risk can be a good estimate of real generalization ability of the tested algorithm, especially when the whole cross-validation is performed several times (each time with different data split) and n is appropriately chosen. To get a good estimate of generalization ability of a learning machine, it is important to analyse not only the average test error, but also its variance, which can be seen as a measure of stability.
We found out, that comparison of the 10-fold cross-validation error is not stable enough to decide, which configuration of the classifier is better. Therefore we used 10 fold 10 cross-validation setup and calculated classification errors in each step of 10 fold 10 cross-validation for each classifier. A mean value of the classification error was calculated from these errors in 10 fold cross-validation and was taken as representation of the classification results for partial classifier. The comparison of the classifiers was done using these mean errors.

Group of Adaptive Model Evolution

Group of Adaptive Models Evolution (GAME) (Kordík, 2005) proceeds from the Group Model Data Handling (GMDH) theory (Ivakhnenko, 1971). GMDH was designed to automatically generate model of the system in the form of polynomial equations. An example of inductive model created by GAME algorithm is depicted in the Figure 9. Similarly to Multi-Layered Perceptron (MLP) neural networks, GAME units (neurons) are connected in a feedforward network (model). The structure of the model is evolved by special niching genetic algorithm, layer by layer. Parameters of the model (coefficients of units' transfer functions) are optimized independently (Kordík et al., 2007). Model can be composed of units of different transfer function type (e.g sigmoid, polynomial, sine, linear, exponential, rational, etc). Units with transfer function performing well on given data set survive the evolution process and form the model. Often, units of several different types survive in one model, making it hybrid.
Here in the chapter, we using GAME models as predictors (continuous output variable) and also as classifiers (four output classes). The evolutionary design of the GAME algorithm makes this possible without need to change the learning strategy. For classification purposes, the GAME model consists mainly of units with sigmoid transfer function and for regression, polynomial, linear or exponential units are often selected to fit the input-output relationship.

Data analysis

The character of the used data set, particularly the uncertain boundary of middle classes excludes the possibility to classify into 10 classes of fractionation with reasonable error. Even for classification into four classes, we got perfect (95%) accuracy for class 1 and 4 only, the accuracy for other two classes was bad (around 65%). Reflecting these preliminary experiments we projected the data into two dimensions (using (Drchal et al., 2007)) and found

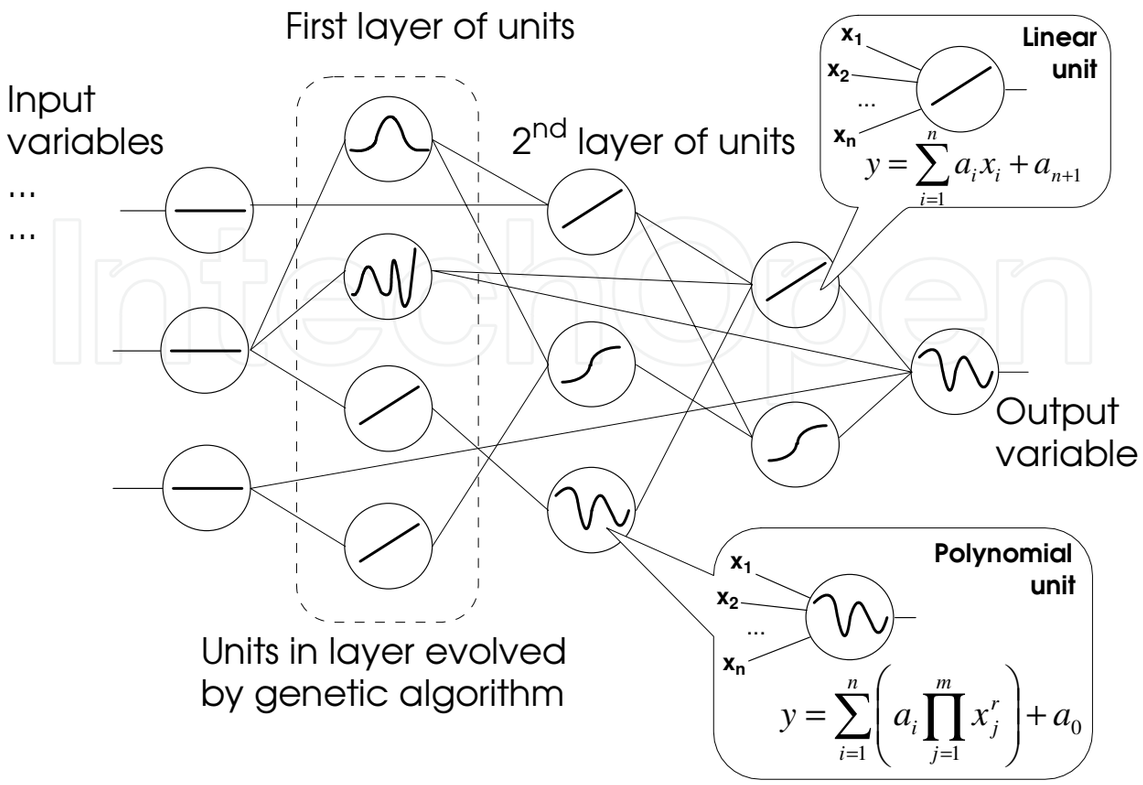

Fig. 9. The structure of the GAME model is evolved layer by layer using special genetic algorithm. While training a unit, selected optimization method adjusts coefficients $(a_1, ..., a_n)$ in the transfer function of the unit.

boundaries better separating the data vectors. We prepared two versions of the data set. The first was A-EGM-regression data set, where the output was continuous number taken from raw dataset (not using CF classified by experts). The second was A-EGM-classification data set with three output classes: (1 – organized atrial activity; 2 – intermediate; 3 – high degree of fractionation), where for class one the average one particular A-EGM signal classification (ACF - average class of fractionation) by three experts was below 1.9, for class two the ACF in $\langle 1.9, 3 \rangle$ interval and for the class three the ACF was above 3.

Results of GAME approach

At first, we studied the regression performance of GAME models produced by different configurations of the algorithm. The target variable was the average A-EGM signal ranking by three experts (the A-EGM-regression data set). We found out, and it is also apparent in the box-plot charts, that comparison of the 10 fold cross validation error is not stable enough to decide, which configuration is better. Therefore we repeated the 10 fold cross validation ten times, each time with different fold splitting. For each box plot it was necessary to generate and validate hundred models.

For all experiments we used three default configurations of the GAME algorithm available in FAKE GAME environment (*The FAKE GAME environment for the automatic knowledge extraction*, 2008). The *std* configuration uses just subset of units (those with implemented analytic gradient for faster optimization). It evolves 15 units for 30 epochs in each layer. The *quick*

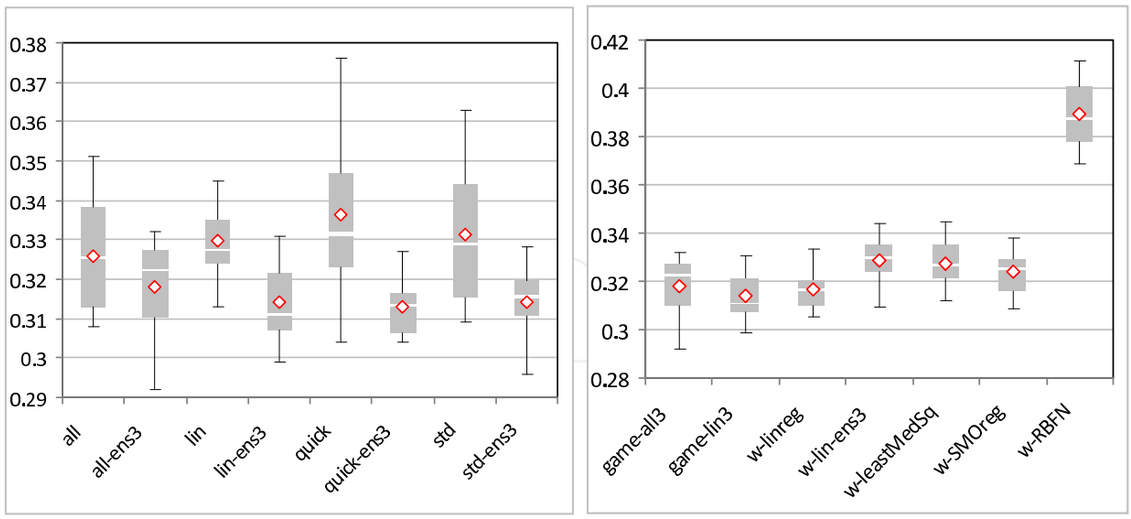

Fig. 10. The comparison of RMS cross validation errors for several configuration of the GAME engine (left). Selected GAME models compared with models generated in WEKA environment (right).

configuration is the same as *std* except that it does not use the niching genetic algorithm (just 15 units in the initial population). The *linear* configuration restricts type of units that can be used to linear transfer function units. The *all* configuration is the same as *std* configuration, in addition it uses all units available in the FAKE GAME environment. This configuration is more computationally expensive, because it also optimizes complex units such as BPNetwork containing standard MLP neural network with the back-propagation of error (Mandischer, 2002).

The GAME algorithm also allows to generate ensemble of models (Brown, 2004; Hansen & Salamon, 1990). Ensemble configurations contain digit (number of models) in their name.

The Figure 10 shows that the regression of the ACF output is not a very difficult task. All basic GAME configurations performed similarly (left chart) and ensembling of three models further improved their accuracy. The ensemble of three linear models performed best in average, but the difference from $all - ens3$ configuration is not statistically significant.

In WEKA data mining environment, *LinearRegression* with embedded feature selection algorithm was the best performing algorithm. Ensembling (bagging) did not improved results of generated model, quite the contrary. The Radial Basis Function Network (RBFN) failed to deliver satisfactory results in spite of experiments with its optimal setting (number of clusters).

Secondly, our experiments were performed on the A-EGM-classification data set. The methodology remained the same as for regression data. Additionally we tested classification performance of 5 models ensembles. Figure 11 left shows that the classes are not linearly separable – *linear* configuration generates poor classifiers and ensembling does not help. Combining models in case of all other configurations improves the accuracy. For *all* configuration the dispersion of cross validation errors is quite high. The problem is in the configuration of the genetic algorithm – with 15 individuals in the population some "potentially useful" types of units do not have chance to be instantiated. Ensembling models generated by this configuration improves their accuracy significantly.

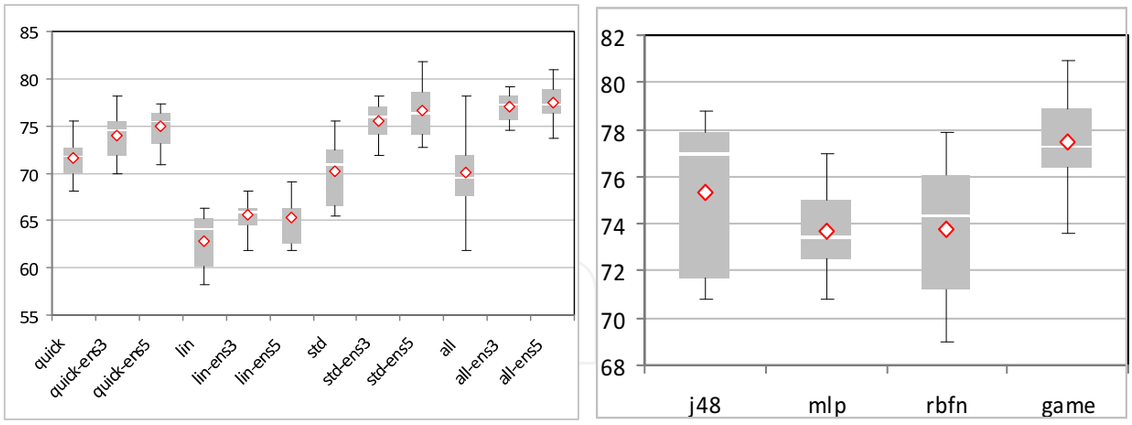

Fig. 11. Classification accuracy in percent for several GAME configurations (left) and comparison with Weka classifiers (right).

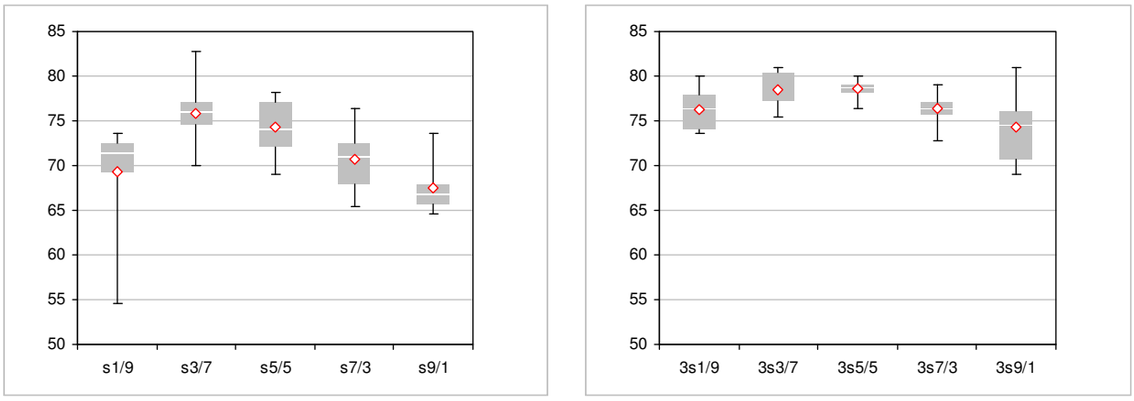

Fig. 12. Classification performance for different ratios of training/validation data split. Left – results for single game models generated by *std* configuration. Right – results for GAME ensemble ($std - ens3$).

Comparison with WEKA classifiers (Figure 11 right) shows that GAME ensemble significantly outperforms Decision Trees (j48), MultiLayered Perceptron (mlp) and Radial Basis Function network (rbfn) implemented in WEKA data mining environment.
The last experiment (Figure 12) showed that the best split of the training and validation data set is $\frac{40\%}{60\%}$ (training data are used by optimization method to adjust parameters of GAME units transfer functions, whereas from validation part, the fitness of units is computed).
Implicitly, and in all previous experiments, training and validation data set was divided $\frac{70\%}{30\%}$ in the GAME algorithm. Changing the implicit setting to $\frac{40\%}{60\%}$ however involves additional experiments on different data sets.

Conclusion of GAME approach classification
Our results showed, that extracted features for CFAEs bear significant information allowing us to classify signals into three classes of fractionation with 80% accuracy for ACF and raw dataset. That is good result with respect to 60% of consistent assignments into four

CF performed by three independent experts. For this data set, the GAME algorithm outperformed well established methods in both classification and regression accuracy. What is even more important, both winning configurations were identical $all - ens$.

6. Discussion and conclusion

Described methodology of the signal processing allowed us to construct several systems that can effectively work with the A-EGM signal in real-time. Figure 13 shows the whole signal path from its recording by catheter touching the endocardial tissue, through the robust wavelet based filtering method, feature extraction and selection phase towards the regression or classification. The result of regression or classification can be then used as a number (color shade) to be mapped into real electro-anatomical maps during the ablation of AF.

In the era of catheter ablation of AF, the initial attempts to describe A-EGMs during AF were predominantly based on frequency-domain analysis of atrial signals (Sanders et al., 2005), (Lazar et al., 2004) and (Lin et al., 2006). Wave morphology similarity approach was alternatively investigated (Ravelli et al., 2005). The pitfalls of spectral mapping have been recently recognized (Ng et al., 2006) and (Ng et al., 2007). Besides technical difficulties, it soon became clear that not only dominant frequency (DF) but also the level of fractionation is clinically important descriptor of local atrial signal (Nademanee et al., 2004) and (Takahashi et al., 2008). Both characteristics are often concordant. Sites with highly fractionated A-EGMs almost fully encompass the sites with high DF but not always vice versa. For that reason, algorithms implemented in commercially available mapping systems were designed for detection of CFAEs rather than high DF (Scherr et al., 2007) and (Verma et al., 2008). These time-domain algorithms require specific input parameters being more flexible but, on the other hand, operator-dependent. In addition, relatively simple mathematical definition of fractionation in those algorithms suggests that more sophisticated analytical methods may provide better performance in CFAEs detection.

Our study showed for the first time that wavelet-based approach to the description of endocardial A-EGMs during AF offers fractionation indexes and classifiers which tightly correlate with the expert classification and have reasonable power to detect highly fractionated A-EGMs. To our best knowledge this is also the first study that utilized atrial signal database and expert ranking to validate automated software algorithm for the quantification of A-EGMs fractionation.

Previous reports on the automated detection of CFAEs showed also promising agreement between CFAEs detection performed automatically and by investigators. In the study by Verma et. al (Verma et al., 2008), the overall agreement between algorithm-labeled (defined as mean cycle length $<$ 120 ms) and investigator-labeled CFAEs sites was 86% for two independent investigators combined. In the study by Wu et. al (Wu et al., 2008), 82.5% of effective sites with significant AF cycle length prolongation after ablation were judged retrospectively as CFAEs sites (defined as shortest cycle interval between $60 - 120$ ms) (Křemen et al., 2008).

Number of A-EGMs in experimental dataset was limited and representative A-EGMs were preselected based on quality from vast amount of data obtained during left-atrial mapping. This could have introduced a bias towards our algorithms. It should be emphasized, however, that fractionation analysis even under "real world conditions" requires much more diligent approach compared to conventional voltage or activation mapping and that higher standards for A-EGM quality are prerequisite for meaningful results. In contrast to DF assessment, stable endocardial contact is crucial for valid fractionation analysis. Consequently, preselection of

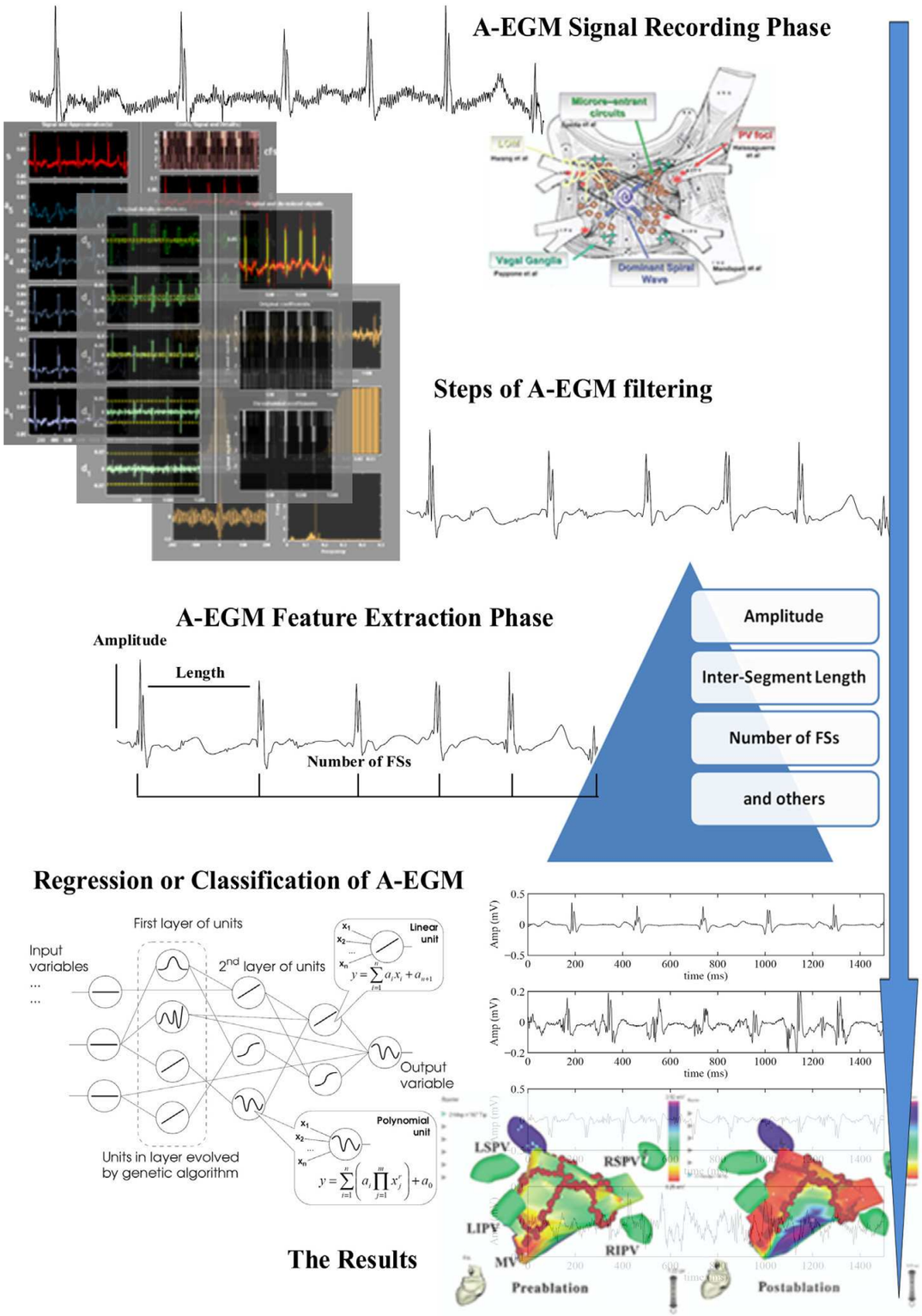

Fig. 13. Schema of described methodology of A-EGM processing and evaluation.

A-EGMs, according to our opinion, is fully appropriate for pilot testing of a new algorithms even if these algorithms are designed quite robustly in order to ensure good performance also for signals with less than optimum signal-to-noise ratio (Křemen et al., 2008).
Some objections may be raised to mere four categories used for expert ranking of A-EGMs. Optimal classification should have been performed in a continuous scale reflecting inherent features of fractionation. However, such classification is difficult to achieve in reasonable time span because of within-expert "drift" in evaluation of consecutive A-EGMs which requires many additional re-evaluation steps. We circumvented this problem by averaging the classification by 3 experts to obtain semi-continuous scale of fractionation (Křemen et al., 2008).
Because of temporal variation in appearance of A-EGMs during AF at some sites, it was shown that the signal assessment requires recording duration > 5 seconds to obtain reproducible fractionation measures Lin et al. (2008) and Stiles et al. (2008). In our study, we used only 1.5 s A-EGMs. This approach seems to be fully adequate because only A-EGMs with stable activation pattern within this period were selected. Assuming that dominant cycle length during AF is usually < 200 ms, the A-EGM duration of 1.5 s covers at least $7 - 8$ signal pattern repetitions which ensures sufficient statistical stability. Temporal alterations of A-EGMs are certainly problematic issue during real-time fractionation mapping but the results of our validation study were not clearly affected by this phenomenon (Křemen et al., 2008).
Our algorithm is fully automatic and does not need any initial settings by the operator like voltage criteria required in CFAEs software of commercially available mapping systems (Scherr et al., 2007) and (Verma et al., 2008) which might be particularly sensitive to background noise and dispersion of voltages at different sites within mapped atrium. Parameter settings in our algorithms were manifold cross-validated using random split of experimental dataset into training and testing subsets. Because correlation between fractionation index and expert classification was chosen as one of the test criterion (instead of CFAEs detection), general performance of algorithms within the whole range of A-EGMs fractionation was confirmed. For all these reasons and because of robust preprocessing steps, the algorithms will hopefully perform well in larger independent sample of A-EGMs with the identical parameter settings. However, this should be a subject of subsequent investigation as well as the definition of cut-off value of indexes of fractionation or classifiers setup for CFAEs detection.
Ablation of CFAEs as adjutant target sites appears to increase success rate of ablation for persistent AF and improves short-term outcome of AF patients as shown in numerous clinical studies. Feasibility of real-time automated detection of CFAEs was investigated, but only in two of studies this feature was directly used for ablation (Verma et al., 2008) and (Porter et al., 2008). So far, any information is missing on the utility of automated assessment of CFAE compared to investigator-based detection in directing the ablation procedure.

7. Acknowledgement

This work was supported by the research projects #*MSM* 6840770012 "Interdisciplinary Biomedical Engineering Research II" from Ministry of Education, Youth and Sports of the Czech Republic and post doctoral research project by Czech Science Foundation GACR #*P*103/11/*P*106.

8. References

Brown, G. (2004). *Diversity in Neural Network Ensembles*, PhD thesis, The University of Birmingham, School of Computer Science, Birmingham B15 2TT, United Kingdom.

Burrus, S. (1997). *Introduction to Wavelets and Wavelet Transforms.*, Prentice Hall.

Daubechies, I. (1992). *Ten lectures on wavelets.*

Donoho, D. (1995). De-noising by soft-thresholding, *IEEE Transactions on Information Theory* 41(3): 613–627.

Drchal, J., Kordík, P. & Šnorek, M. (2007). Dataset Visualization Based on a Simulation of Intermolecular Forces, *IWIM 2007 - International Workshop on Inductive Modelling*, Vol. 1, Czech Technical University in Prague, Praha, pp. 246–253.
URL: *http://cig.felk.cvut.cz*

Faes, L., Nollo, G., Antolini, R., Gaita, F. & Ravelli, F. (2007). A method for quantifying atrial fibrillation organization based on wave morphology similarity, *IEEE Trans Biomed Eng.* 49: 1504–1513.

Faes, L. & Ravelli, F. (2007). A morphology-based approach to the evaluation of atrial fibrillation organization, *IEEE Eng Med Biol Mag.* 26(4): 59–67.

Gustafsson, F. (2000). *Adaptive Filtering and Change Detection*, John Wiley & Sons, Ltd.

Guyon, I., Gunn, S., Nikravesh, M. & Zadeh, L. (2006). *Feature Extraction, Foundations and Applications*, Physica-Verlag, Springer.

Haissaguerre, M., Jais, P., Shah, D., Takahashi, A., Hocini, M., G, Q., Garrigue, S., Le Mouroux, A., Le Metayer, P. & Clementy, J. (2003). Spontaneous initiation of af by ectopic beats originating in the pulmonary veins, *N Engl J Med* 339: 659–666.

Hansen, L. & Salamon, P. (1990). Neural network ensembles, *IEEE Trans. Pattern Anal. Machine Intelligence* 12(10): 993–1001.

Ivakhnenko, A. G. (1971). Polynomial theory of complex systems, *IEEE Transactions on Systems, Man, and Cybernetics* SMC-1(1): 364–378.

Jais, P., Haissaguerre, M., Shah, D., Chouairi, S. & Clementy, J. (1996). Regional disparities of endocardial atrial activation in paroxysmal atrial fibrillation, *Pacing Clin Electrophysiol.* pp. 1998–2003.

Konings, K., Kirchhof, C., Smeets, J., Wellens, H., Penn, O. & Allessie, M. (1994). High-density mapping of electrically induced atrial fibrillation in humans, *Circulation* 89: 1665–1680.

Konings, K., Smeets, J., Penn, O., Wellens, H. & Allessie, M. (1997). Configuration of unipolar atrial electrograms during electrically induced atrial fibrillation in humans, *Circulation* 95: 1231–1241.

Kordík, P. (2005). Game - group of adaptive models evolution, *Technical Report DCSE-DTP-2005-07*, Czech Technical University in Prague, FEE, CTU Prague, Czech Republic.

Kordík, P., Kovářík, O. & Šnorek, M. (2007). OPTIMIZATION OF MODELS: LOOKING FOR THE BEST STRATEGY, *Proceedings of the 6th EUROSIM Congress on Modelling and Simulation*, Vol. 2, ARGESIM, Vienna, pp. 314–320.
URL: *http://neuron.felk.cvut.cz/ kordikp/iw/eurosim07.pdf*

Kosinski, D., Grubb, P., Wolfe, A. & Mayhew, H. (1998). Catheter ablation for atrial flutter and fibrillation an effective alternative to medical therapy, *POSTGRADUATE MEDICINE* 103.

Kottkamp, H. & Hindricks, G. (2007). Complex fractionated atrial electrograms in atrial fibrillation: A promising target for ablation, but why, when and how?, *Heart Rhythm* pp. 1021–1023.

Křemen, V. & Lhotská, L. (2007a). Automatic Search of Individual Signal Complexes in Complex Fractionated Atrial Electrograms Using Wavelet Transform, *8th International Workshop on Mathematical Methods in Scattering Theory and Biomedical Engineering - book of abstracts*, University of Ioannina, Crete, p. 37.

Křemen, V. & Lhotská, L. (2007b). Novel approach to search for individual signal complexes in complex fractionated atrial electrograms using wavelet transform, *6th International Special Topic Conference on ITAB - Proceedings*, IEEE, Piscataway, pp. 83–86.

Křemen, V. & Lhotská, L. (2008). Evaluation of Novel Algorithm for Search of Signal Complexes to Describe Complex Fractionated Atrial Electrogram, *Biosignals 2008 - II.*, Vol. 2, INSTICC Press, Setúbal, pp. 416–419.

Křemen, V., Lhotská, L., Čihák, R., Vančura, V., Kautzner, J. & Wichterle, D. (2008). A new approach to automated assessment of endocardial electrograms fractionation in human left atrium during atrial fibrillation., *Physiol. Measurement* .

Křemen, V., Lhotská, L. & Macaš, M. (2007). Using PSO Algorithm to Optimize Parameters of Time-Domain Method for Complex Fractionated Atrial Electrograms Evaluation , *8th International Workshop on Mathematical Methods in Scattering Theory and Biomedical Engineering - book of abstracts*, University of Ioannina, Crete, p. 36.

Lazar, S., Dixit, S., Marchlinski, F., Callans, D. & Gerstenfeld, E. (2004). Presence of left-to-right atrial frequency gradient in paroxysmal but not persistent atrial fibrillation in humans, *Circulation* 110: 3181–3186.

Lin, Y., Tai, C., Kao, T., Chang, S., Wongcharoen, W., Lo, L., Tuan, T., Udyavar, A., Chen, Y., Higa, S., Ueng, K. & Chen, S. (2008). Consistency of complex fractionated atrial electrograms during atrial fibrillation, *Heart Rhythm* 5: 406–12.

Lin, Y., Tai, C., Kao, T., Tso, H., Higa, S., Tsao, H., Chang, S., Hsieh, M. & Chen, S. (2006). Frequency analysis in different types of paroxysmal atrial fibrillation, *J. Am. Coll. Cardiol.* 47: 1401–1407.

Mallat, S. (1999). *A Wavelet tour of Signal Processing. 2. edition*, Academic Press.

Mandischer, M. (2002). A comparison of evolution strategies and backpropagation for neural network training, *Neurocomputing* (42): 87–117.

Nademanee, K. (2007). Trials and travails of electrogram-guided ablation of chronic atrial fibrillation, *Circulation* 115: 2592–2594.

Nademanee, K., McKenzie, J., Kosar, E., Schwab, M., Sunsaneewitayakul, B., Vasavakul, T., Khunnawat, C. & Ngarmukos, T. (2004). A new approach for catheter ablation of atrial fibrillation: mapping of the electrophysiologic substrate, *J Am Coll Cardiol* 43: 2044–53.

Ng, J., Gold, J. & Goldberger, J. (2007). Understanding and interpreting dominant frequency analysis of af electrograms, *Journal of Cardiovascular Electrophysiology* pp. 680–685.

Ng, J., Kadish, A. & Goldberger, J. (2006). Effect of electrogram characteristics on the relationship of dominant frequency to atrial activation rate in atrial fibrillation, *Heart Rhythm* pp. 1295–1305.

Novak, D. (2003). *Electrocardiogram Signal Processing using Hidden Markov Models*, PhD thesis, Czech Technical University in Prague, Faculty of Electrical Engineering, Technicka 2, 166 27 Prague 6, Czech Republic.

Porter, M., Spear, W., Akar, J., Helms, R., Brysiewicz, N., Santucci, P. & Wilber, D. (2008). Prospective study of atrial fibrillation termination during ablation guided by automated detection of fractionated electrograms., *J. Cardiovasc. Electrophysiol.* . [May 5; electronic publication ahead of print].

Ravelli, F., Faes, L., Sandrini, L., Gaita, F., Antolini, R., Scaglione, M. & Nollo, G. (2005). Wave similarity mapping shows the spatiotemporal distribution of fibrillatory wave complexity in the human right atrium during paroxysmal and chronic atrial fibrillation, *J. Cardiovasc. Electrophysiol.* 16: 1071–1076.

Sanders, P., Berenfeld, O., Hocini, M., Jais, P., Vaidyanathan, R., Hsu, L., Garrigue, S., Takahashi, Y., Rotter, M., Sacher, F., Scavee, C., Ploutz-Snyder, R., Jalife, J. & Haissguerre, M. (2005). Spectral analysis identifies sites of high frequency activity maintaining atrial fibrillation in humans, *Circulation* 112: 789–797.

Scherr, D., Dalal, D., Cheema, A., Cheng, A., Henrikson, C., Spragg, D., Marine, J., Berger, R., Calkins, H. & Dong, J. (2007). Automated detection and characterization of complex fractionated atrial electrograms in human left atrium during atrial fibrillation, *Heart Rhythm* 4: 1013–1020.

Stiles, M., Brooks, A., John, B., Shashidhar, Wilson, L., Kuklik, P., Dimitri, H., Lau, D., Roberts-Thomson, R., Mackenzie, L., Willoughby, S., Young, G. & Sanders, P. (2008). The effect of electrogram duration on quantification of complex fractionated atrial electrograms and dominant frequency, *J. Cardiovasc. Electrophysiol.* 19: 252–258.

Takahashi, Y., OŃeill, M., Hocini, M., Dubois, R., Matsuo, S., Knecht, S., Mahapatra, S., Lim, K., Jais, P., Jonsson, A., Sacher, F., Sanders, P., Rostock, T., Bordachar, P., Clementy, J., Klein, G. & Haissaguerre, M. (2008). Characterization of electrograms associated with termination of chronic atrial fibrillation by catheter ablation., *J. Am. Coll. Cardiol.* 51: 1003–1010.

The FAKE GAME environment for the automatic knowledge extraction (2008). available online at: http://www.sourceforge.net/projects/fakegame.

Verma, A., Novak, P., Macle, L., Whaley, B., Beardsall, M., Wulffhart, Z. & Khaykin, Y. (2008). A prospective multicenter evaluation of ablating complex fractionated electrograms (CFEs) during atrial fibrillation (AF) identified by an automated mapping algorithm: acute effects on AF and efficacy as an adjuvant strategy, *Heart Rhythm* 5: 198–205.

Wu, J., Estner, H., Luik, A., Ucer, E., Reents, T., Pflaumer, A., Zrenner, B., Hessling, G. & Deisenhofer, I. (2008). Automatic 3D mapping of complex fractionated atrial electrograms (CFAE) in patients with paroxysmal and persistent atrial fibrillation., *J. Cardiovasc. Electrophysiol.* . [March 28; electronic publication ahead of print].

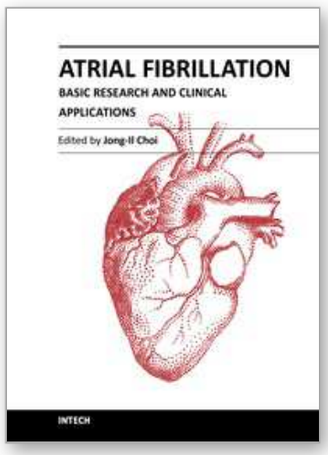

Atrial Fibrillation - Basic Research and Clinical Applications

Edited by Prof. Jong-Il Choi

ISBN 978-953-307-399-6
Hard cover, 414 pages
Publisher InTech
Published online 11, January, 2012
Published in print edition January, 2012

Atrial Fibrillation-Basic Research and Clinical Applications is designed to provide a comprehensive review and to introduce outstanding and novel researches. This book contains 22 polished chapters and consists of five sections: 1. Basic mechanisms of initiation and maintenance of atrial fibrillation and its pathophysiology, 2. Mapping of atrial fibrillation and novel methods of signal detection. 3. Clinical prognostic predictors of atrial fibrillation and remodeling, 4. Systemic reviews of catheter-based/surgical treatment and novel targets for treatment of atrial fibrillation and 5. Atrial fibrillation in specific conditions and its complications. Each chapter updates the knowledge of atrial fibrillation, providing state-of-the art for not only scientists and clinicians who are interested in electrophysiology, but also general cardiologists.

How to reference

In order to correctly reference this scholarly work, feel free to copy and paste the following:

Vaclav Kremen and Lenka Lhotska (2012). Digital Signal Processing and Artificial Intelligence Methods for Intracardial Signal Complexity Evaluation, Atrial Fibrillation - Basic Research and Clinical Applications, Prof. Jong-Il Choi (Ed.), ISBN: 978-953-307-399-6, InTech, Available from: http://www.intechopen.com/books/atrial-fibrillation-basic-research-and-clinical-applications/digital-signal-processing-and-artificial-intelligence-methods-for-intracardial-signal-complexity-eva

INTECH
open science | open minds

InTech Europe
University Campus STeP Ri
Slavka Krautzeka 83/A
51000 Rijeka, Croatia
Phone: +385 (51) 770 447
Fax: +385 (51) 686 166
www.intechopen.com

InTech China
Unit 405, Office Block, Hotel Equatorial Shanghai
No.65, Yan An Road (West), Shanghai, 200040, China
中国上海市延安西路65号上海国际贵都大饭店办公楼405单元
Phone: +86-21-62489820
Fax: +86-21-62489821

IntechOpen